Desalination and Water Treatment
www.deswater.com

doi: 10.5004/dwt.2022.27964

246 (2022) 36–53
January

An investigation on effect of dissimilarity of mass flow rate on hourly, daily and annual efficiencies of double slope type solar still included with N similar PVT compound parabolic concentrators

Vivek Singh[a,b], Rakesh Kumar[a], Desh Bandhu Singh[c,*]

[a]*Department of Mechanical Engineering, Indian Institute of Technology (ISM) Dhanbad, Jharkhand, India, emails: vsingh.ald@gmail.com (V. Singh), rakesh@iitism.ac.in (R. Kumar)*
[b]*Galgotias College of Engineering and Technology, Plot No. 1, Knowledge Park II, Greater Noida 201306, Uttar Pradesh, India, email: vsingh.ald@gmail.com*
[c]*Department of Mechanical Engineering, Graphic Era Deemed to be University, Bell Road, Clement Town, Dehradun – 248002, Uttarakhand, India, email: deshbandhusingh.me@geu.ac.in/dbsiit76@gmail.com*

Received 24 July 2021; Accepted 4 November 2021

ABSTRACT

In this research work, an investigation on effect of dissimilarity of mass flow rate on hourly, daily and annual efficiencies of double slope type solar still included with N similar PVT compound parabolic concentrators keeping water depth as 0.14 m has been carried out. All four kinds of weather situations have been incorporated for estimation of annual performance parameters. The relevant data have been accessed from Indian Meteorological Department situated at Pune in India. Data and equations have been fed to computer code inscribed in MATLAB-2015a for getting values of parameters for different values of mass flow rate keeping number of collectors constant to know the effect of dissimilarity of mass flow rate on annual efficiency of the proposed system. It has been concluded that the value of annual efficiency decreases with the enhancement in the value of mass flow rate at given water depth and number of collectors till mass flow rate = 0.10 kg/s and then become almost constant.

Keywords: Annual efficiency; Mass flow rate; Active solar still; Compound parabolic concentrators

1. Introduction

The design, analysis and installation of solar energy based solar still for generating fresh water is the need of time because the world is facing with the scarcity of fresh water. Solar still uses greenhouse effect for the generation of distilled water using solar energy and the device named solar still is self-sustainable and hence it can be installed and operated in remote location for the generation of fresh water for different use. The solar still is generally classified as passive and active types. Passive type solar still produces fresh water in the range of 1–3 kg/m^2 which is low and this low generation of fresh water can be overcome by integrating heat supplying system that will supply heat to basin resulting in the enhancement in the temperature of water in the basin. This type of solar still having heat supplying arrangement is known as active solar still. The output of active is competitive and it can be used for supplying fresh water on commercial level. The active type of solar still which is also known as solar energy operated water purifier (SEOWP) in active mode was first introduced by Rai and Tiwari in 1983. Since then, a lot of advancements have been reported around the globe by different researchers which have been summarized in paragraphs that follow.

* Corresponding author.

Rai and Tiwari [1] reported the enhancement in fresh water yielding of SEOWP by incorporating one conventional flat plate collector (FPC) over passive type SEOWP of the same basin area due to the supply of heat to the basin in active mode of operation. This water purifier was not self-sustainable as the pump needed some electric power for working which was supplied through grid. The active type SEOWP in the forced mode of operation can be made self-sustainable by incorporating solar panel. Kumar and Tiwari [2] proposed the integration of PVT with FPC for supplying heat to basin of passive type SEOWP taking inspiration from the work of Kern and Russell [3]. It was reported by Kern and Russell that the electrical efficiency of solar panel got increased upon integration of solar panel with solar collector due the removal of heat by fluid passing below the panel. Kumar and Tiwari reported the improvement in output by 3.5 times over the similar passive type SEOWP due to the addition of heat by two collectors in which only one of them was integrated with PVT for making the system self-sustainable. The work of Kumar and Tiwari was extended by Singh et al. [4] for DS type SEOWP in active mode. Further, Singh et al. [5] and Tiwari et al. [6] reported the experimental investigation of SEOWP by incorporating two FPCs in which both FPCs were partially integrated with PVT. They reported an enhancement in DC electrical output; however, the yield of fresh water was less as compared to the system reported by Kumar and Tiwari [2]. Heat gain was less because more area of FPCs was covered by PVT. Further, active type SEOWP was studied under optimized situation [7–11]. It was reported that the DS type SEOWP under optimized condition by incorporating N alike PVT-FPCs had 74.66% higher energy payback time (ENPBT) over passive type DS-SEOWP. The value of exergoeconomic parameter for single slope type SEOWP was found to be 47.37% higher than the passive type single slope SEOWP of same basin area. Sahota et al. [12] reported the use of nanofluid in DS type SEOWP in active mode for enhancing the fresh water output.

Carranza et al. [13] have experimentally investigated the performance of DS type SEOWP loaded with nanofluid by incorporating preheating of saline water and concluded that water yield increases due to better thermophysical properties of nanofluid as compared to base fluid. Kouadri et al. [14] have investigated solar still by incorporating zinc and copper oxides for the location of Algeria and compared the yield with conventional SEOWP and concluded that the water yield was improved by 79.39% due to having better thermophysical characteristic of nanofluid. The output of SEOWP could further be enhanced by changing the design of solar collector which could absorb higher amount of heat from the sun or by changing the design of solar still. PVT integrated FPC could gain higher heat if some concentrating part was integrated with FPC. With this concept in mind, Atheaya et al. [15] proposed PVT integrated compound parabolic concentrator collector (CPC) and reported its thermal model which was further extended by Tripathi et al. [16] for N collectors connected in series and loop was opened. Singh and Tiwari [17–19], Gupta et al. [20,21], Singh et al. [22,23] and Sharma et al. [24] investigated SEOWP of basin type by incorporating characteristic equations development and concluded that SEOWP of double slope type performs better than SEOWP of single slope type under optimized conditions of mass flow rate ($\dot{m}_f$) and number of collectors (N) at 0.14 m water depth due to better distribution of solar energy in the case of DS type. Prasad et al. [25], Bharti et al. [26], Singh [27] investigated SEOWP of double slope type from sensitivity viewpoint and concluded that the sensitivity analysis helps designer and installer of solar systems as which parameter should be focused more for a particular application.

The heat gain by solar collector can be enhanced by providing evacuated tubes because convection loss does not take place through vacuum. Sampathkumar et al. [28] investigated the SEOWP by incorporating evacuated tubular collector and reported an increase of 129% over the SEOWP of the same basin area due to the addition of heat to the basin by collectors. An investigation of SEOWP in natural mode of operation by incorporating evacuated tubes was done by Singh et al. [29] and reported exergy efficiency lying in the range of 0.15% to 8%. Further, an investigation of SEOWP incorporated with evacuated tubes was done in forced mode of operation by inserting pump between collector and basin and reported enhanced fresh water output as compared to the similar system operated in natural mode due to better circulation of fluid in the forced mode of operation [30]. Mishra et al. [31] reported characteristic equation development for N alike series connected ETCs. The work reported by Mishra et al. [31] was further extended by Singh et al. [32–34]. The thermal modeling of basin type SEOWP by incorporating N alike ETCs was reported by them and comparison was also made between single slope active water purifier and DS type SEOWP in active mode taking energy, exergy, energy metrics, exergoeconomic and enviroeconomic parameters as basis. Issa and Chang [35] further extended the work of Singh et al. by connecting ETCs in mixed mode of operation experimentally and reported enhanced output as compared to similar set up in passive mode due to heat addition by collectors in active mode. Moreover, Singh and Al-Helal [36], Singh [37] and Sharma et al. [38,39] reported development of characteristic equations and the observations based on the energy metrics for SEOWP by incorporating evacuated tubular collector as well as compound parabolic concentrator integrated evacuated tubular collector.

Patel et al. [40–42] have reviewed recently SEOWP included with various kinds of collectors. Further, Singh et al. [43] reviewed SEOWP included with various kinds of collectors and loaded with nanofluid with an aim to find the effect of nanofluid on the performance of active SEOWP. Nanofuid is obtained by mixing a small amount of nanoparticles to water. The effect of adding nanoparticles to water in SEOWP is to increase the output (potable water and exergy) of SEOWP. The better performance of nanofluid loaded SEOWP than loaded with water is due to the possession of better thermo-physical characteristic of nanofluid as compared to water. Bansal et al. [44] have reported the mini review of changing the material of absorber on the performance of solar still. Shankar et al. [45] have studied ETC integrated SEOWP in natural as well forced mode and concluded that forced mode is better for environment as higher carbon credit was observed in forced mode due to more addition of heat to basin in the case of forced mode.

Abdallah et al. [46] have investigated spherical and pyramid basin SEOWP and concluded that the spherical basin SEOWP gave 57.1% higher water yield due to better utilization of solar radiation in the case of spherical basin.

Essa et al [47] studied vertical solar still with rotating disc and it was concluded that the best performance was obtained at 1.5 rpm. Elaziz et al. [48] studied ensemble random vector functional link networks for predicting the fresh water yielding from active solar stills loaded with nanoparticles. The predicted results were validated with experimental data and coefficient of determinations were found as 0.982 and 0.991for copper and aluminum oxides nanofluids respectively. Hassan et al. [49] have studied single slope type solar still included with parabolic trough collectors and it was reported that the inclusion of parabolic trough collectors resulted in improved energy payback time and unit cost of fresh water yielding as compared to conventional solar still. Thakur et al. [50] have studied solar still included with parabolic trough collector by incorporating carbon pellets and it was concluded that the daily yield was 85.2% higher than the conventional solar still due to synergetic effect of collector and porous carbon.

From the extant research, it is seen that the effect of mass flow rate ($\dot{m}_f$) on various efficiencies of double slope type solar still included with N similar PVT compound parabolic concentrators (NPVTCPC-DS) has not been reported by any researcher. Hence, this work focuses on the study of effect of dissimilarity of mass flow rate on the various annual efficiencies of NPVTCPC-DS. The various efficiencies considered are thermal, exergy, electrical, overall exergy and overall thermal efficiencies on per annum basis. The difference between the earlier reported work and the proposed work lies in the fact that the efficiency and productivity of active type SEOWP was computed at a fixed value of $\dot{m}_f$ as well as N; whereas, in the proposed work, the efficiency of NPVTCPC-DS has been estimated by varying values of $\dot{m}_f$. It has been tried to find the suitable values of $\dot{m}_f$ taking various annual efficiencies as the basis.

2. System metaphors

The specification of NPVTCPC-DS has been revealed as Table 1. Fig. 1 represents NPVTCPC-DS set up. It consists of series connected N similar PVTCPCs, pump and double slope (DS) type SEBWP. The setup incorporates series connected N number of PVTCPCs to SEBWP of double slope type with the help of pump. Pump gets its power from grid for its working. Collectors are connected in series with the help of insulated pipe, the output of last collector is connected to basin through insulated pipe and input to the first collector has also been taken through insulated pipe from pump which takes water from basin through insulated pipe. One collector has a surface area of 1 m^2 hence the total surface area of the sequence of evacuated tubular collectors is N m^2. PVTCPCs are connected in series to a double slope type SEBWP basin with 2 m × 1 m (2 m^2) basin area. It can be fabricated using galvanized iron (GI) sheet. The inside surface of GI sheet can be painted black to absorb solar radiation. The outer surface can be covered with glass wool and thermocol. The top surface of double slope type SEBWP was covered with glass having angle of inclination as 15° as the setup has been designed for summer season viewpoint. The glass can be fixed with help of iron clamp and rubber placed in between iron frame and glass. The sealing can be done using window-putty with an aim to avoid seepage of vapor. The short wavelength solar radiation reaches the water surface after passing through the condensing cover where a part of energy is reflected by

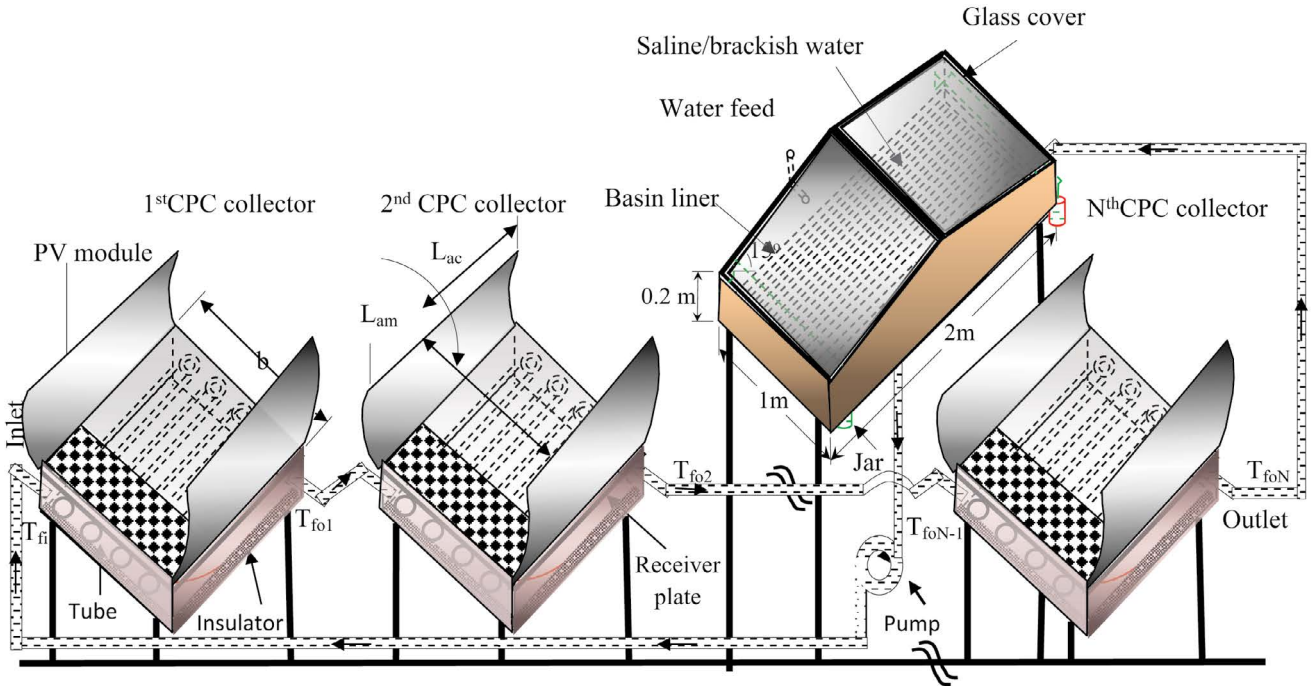

Fig. 1. Schematic diagram of NPVTCPC-DS in which collectors are having series connection.

Table 1
Specifications of NPVTCPC-DS

Component	Specification	Component	Specification
DS type solar still			
Length	2 m	Orientation	East-West
Width	1 m	Thickness of glass cover	0.004 m
Inclination of glass cover	15°	K_g	0.816 W/m-K
Height of smaller side	0.2 m	Thickness of insulation	0.1 m
Material of body	GRP	Thermal conductivity of insulation	0.166 W/m-K
Material of stand	GI		
Cover material	Glass		
PVT-CPC collector			
Type and number of collectors	Tube in plate type, N	Aperture area	2 m^2
Receiver area of solar water collector	1.0 m × 1.0 m	Aperture area of module	0.5 m × 2.0 m
Collector plate thickness	0.002 m	Aperture area of receiver	0.75 m × 2.0 m
Thickness of copper tubes	0.00056 m	Receiver area of module	0.25 m × 1.0 m
Length of each copper tubes	1.0 m	Receiver area of collector	0.75 m × 1.0 m
K_i (Wm^{-1} K^{-1})	0.166	F'	0.968
FF	0.8	ρ	0.84
Thickness of insulation	0.1 m	τ_g	0.95
Angle of CPC with horizontal	30°	α_c	0.9
Thickness of toughen glass on CPC	0.004 m	β_c	0.89
Effective area of collector under glass	0.75 m^2	α_p	0.8
Pipe diameter	0.0125 m	Effective area of collector	0.25 m^2
DC motor rating	12 V, 24 W	under PV module	

water and the remainder is transmitted to the basin liner after being absorbed by water. The basin liner transmits the absorbed energy to the water as it is insulated from outside, and loss of heat is not possible to outside. The temperature of the water within the solar still increases and the heat transfer from the water surface to condensing cover takes place via convection, radiation and evaporation. Water vapor condenses at the inside surface of the cover after losing latent heat of condensation, and film wise condensation can be ensured by careful cleaning of the surface so that condensate can be collected as it will trickle down due to the component of gravity force. Drop wise condensation has negative effect on the performance of solar still as it will not allow the solar radiation to pass through it, that is, it will act as opaque surface to incoming solar radiation. The heat accumulated at the condensing glass surface is dissipated to the surrounding by means of convection and radiation and it strongly depends on the wind speed or water flow rate if additional arrangement is made to dissipate it in the form of water flow over condensing cover over a certain time period. The distillate can be collected in a jar.

3. Mathematical modeling based on energy balance equations

Mathematical modeling of NPVTCPC-DS means writing equations for all its components by equating input energy to output energy. Following assumptions presented in Singh and Tiwari [19], the mathematical modeling for the proposed system can be done as follows:

3.1. Heat gain for N equal partially covered PVTCPCs

The heat gain from N equal partially covered PVTCPCs and temperature at the outlet of last collector can be written as follows [16]:

$$\dot{Q}_{uN} = \frac{\left(1-K_k^N\right)}{\left(1-K_k\right)}\left(AF_R\left(\alpha\tau\right)\right)_1 I_b\left(t\right) + \frac{\left(1-K_k^N\right)}{\left(1-K_k\right)}\left(AF_RU_L\right)_1\left(T_{\text{fi}}-T_a\right) \quad (1)$$

$$T_{\text{foN}} = \frac{I_b\left(t\right)\left(AF_R\left(\alpha\tau\right)\right)_1}{\dot{m}_fC_f}\frac{\left(1-K_k^N\right)}{\left(1-K_k\right)} + \frac{T_a\left(AF_RU_L\right)_1}{\dot{m}_fC_f}\frac{\left(1-K_k^N\right)}{\left(1-K_k\right)} + T_{\text{fi}}K_k^N \quad (2)$$

where $T_{\text{fi}} = T_w$. NPVTCPCs are in closed loop in the proposed water purifier as the fluid at the outlet of last collector is allowed to flow to the basin of solar still. Hence, $T_{\text{wo}} = T_{\text{foN}}$.

The electrical efficiency of solar cells (η_{cN}) of NPVTCPCs can be expressed as [51,52]:

$$\eta_{\text{cN}} = \eta_o\left[1-\beta_o\left(\bar{T}_{\text{cN}}-T_o\right)\right] \quad (3)$$

where η_o stands for efficiency under standard state test condition and $\bar{T}_{\text{cN}}$ stands for average value of temperature of solar cell of NPVTCPCs.

3.2. For DS type solar still

The equation based on equating input and output energies for different components of DS type solar still can be inscribed and these equations can further be simplified using equation (1) following the principle of mathematics and expression for water temperature (T_w) as a function of time can be written as [19]:

$$T_w = \frac{\overline{f_1}(t)}{a_1}\left(1 - e^{-a_1 t}\right) + T_{w0}e^{-a_1 t} \tag{4}$$

where T_{w0} is the temperature of water at the initial condition (t = 0) and $\overline{f_1}(t)$ is the average value of $f_1(t)$ over the time interval from 0 to t. Once T_w is computed from Eq. (4), one can compute the temperature of inner and outer surface of glass cover (T_{giE}, T_{goE}, T_{giW} and T_{goW}) as [19]:

$$T_{giE} = \frac{A_1 + A_2 T_w}{P} \tag{5}$$

$$T_{giW} = \frac{B_1 + B_2 T_w}{P} \tag{6}$$

$$T_{goE} = \frac{\frac{K_g}{L_g}T_{giE} + h_{1gE}T_a}{\frac{K_g}{L_g} + h_{1gE}} \tag{7}$$

$$T_{goW} = \frac{\frac{K_g}{L_g}T_{giW} + h_{1gW}T_a}{\frac{K_g}{L_g} + h_{1gW}} \tag{8}$$

The different unknown terms in Eqs. (1)–(8) are given in Appendix-A. The fresh water yielding from NPVTCPC-DS can be written as:

$$\dot{m}_{ew} = \left[\frac{h_{ewE}\frac{A_b}{2}\left(T_w - T_{giE}\right) + h_{ewW}\frac{A_b}{2}\left(T_w - T_{giW}\right)}{L}\right] \times 3{,}600 \tag{9}$$

4. Analysis

For the analysis of the effect of $\dot{m}_f$ on the various efficiencies of NPVTCPC-DS, 4 climatic situations for each month of year have been taken. These climatic situations can be defined by number of sunshine hours (N') and daily diffuse to daily global irradiation ratio (r') as follows:

- Clear day (blue sky) $r' \le 0.25$ and $N' \ge 9$ h
- Hazy day (fully) $0.25 \le r' \le 0.50$ and $7\text{ h} \le N' \le 9\text{ h}$
- Hazy and cloudy (partially) $0.50 \le r' \le 0.75$ and $5\text{ h} \le N' \le 7\text{ h}$
- Cloudy day (fully) $r' \ge 0.75$ and $N' \le 5$ h

4.1. Energy estimation

The expression of overall annual energy (E_{out}) for NPVTCPC-DS considering first law of thermodynamics can be expressed as:

$$E_{out} = \frac{\left(M_{ew} \times L\right)}{3{,}600} + \frac{\left(P_m - P_u\right)}{0.38} \tag{10}$$

where M_{ew} is annual potable water yielding obtained from NPVTCPC-DS, P_m is yearly electrical power received from PVT, P_u is yearly electrical power utilized by pump and L is latent heat. Here, factor 0.38 which is present in the denominator converts electrical energy into heat. This factor is basically the efficacy of power output taken from conventional power plant [53].

The hourly electrical energy ($\dot{E}x_e$) for the solar panel used in NPVTCPC-DS can be expressed as follows:

$$\dot{E}x_e = A_m I_b(t)\sum_{1}^{N}\left(\alpha\tau_g\eta_{cN}\right) \tag{11}$$

Eq. (11) can be used for evaluating daily electrical exergy of type (a) climatic situation by summing the hourly value of 10 h because the solar flux exists for 10 h only. The similar approach has been used to work out the daily electrical exergy for rest types of climatic situation, that is, type (b) to type (d). The value of electrical exergy on monthly basis for type (a) climatic situation has been evaluated as the multiplication of electrical exergy on daily basis and the corresponding value of number of clear days (n'). The similar approach has been used to work out the electrical exergy on monthly basis for rest types of climatic situation, that is, type (b) to type (d). The value of net electrical exergy on monthly basis has been worked out by summing electrical exergies values for type (a) to type (d) climatic situations. The value of electrical energy (P_m) on annual basis has been worked out by the summing of electrical energy on monthly basis for 12 months. The similar approach has been followed for the estimation of annual fresh water yielding (M_{ew}).

4.2. Exergy estimation

The exergy of NPVTCPC-DS has been estimated using first and second laws of thermodynamics. The hourly output thermal exergy ($\dot{E}x_{out}(W)$) for N-PVT-CPC-DS can be estimated as [54]:

$$\dot{E}x_{out} = h_{ewgE} \times \frac{A_b}{2} \times \left[\left(T_w - T_{giE}\right) - (T_a + 273) \times \ln\left\{\frac{(T_w + 273)}{\left(T_{giE} + 273\right)}\right\}\right] + h_{ewgW} \times \frac{A_b}{2} \times \left[\left(T_w - T_{giW}\right) - (T_a + 273) \times \ln\left\{\frac{(T_w + 273)}{\left(T_{giW} + 273\right)}\right\}\right] \tag{12}$$

where

$$h_{e,wg} = 16.273 \times 10^{-3} h_{c,wg}\left[\frac{P_w - P_{gi}}{T_w - T_{gi}}\right] \text{ [55]} \tag{13}$$

$$h_{c,\mathrm{wg}} = 0.884\left[\left(T_w - T_{\mathrm{gi}}\right) + \frac{\left(P_w - P_{\mathrm{gi}}\right)\left(T_w + 273\right)}{268.9\times10^3 - P_w}\right]^{\left(\frac{1}{3}\right)} \quad [56] \tag{14}$$

$$P_w = \exp\left[25.317 - \frac{5{,}144}{\left(T_w + 273\right)}\right] \tag{15}$$

and

$$P_{\mathrm{gi}} = \exp\left[25.317 - \frac{5{,}144}{\left(T_{\mathrm{gi}} + 273\right)}\right] \tag{16}$$

Eq. (12) can be used for evaluating daily thermal exergy of type (a) climatic situation by summing the hourly value of 10 h because the solar flux exists for 10 h only. The similar approach has been used to work out the daily thermal exergy for rest types of climatic situation, that is, type (b) to type (d). The value of thermal exergy on monthly basis for type (a) climatic situation has been evaluated as the multiplication of thermal exergy on daily basis and the corresponding value of number of clear days (n'). The similar approach has been used to work out the thermal exergy on monthly basis for rest types of climatic situation, that is, type (b) to type (d). The value of net thermal exergy on monthly basis has been worked out by summing thermal exergies values for type (a) to type (d) climatic situations. The value of thermal exergy on annual basis has been worked out by the summing of thermal energy on monthly basis for 12 months.

The value of yearly overall annual exergy gain ($G_{\mathrm{ex,annual}}$) for NPVTCPC-DS has been expressed as follows:

$$G_{\mathrm{ex,annual}} = \mathrm{Ex}_{\mathrm{out}} + \left(P_m - P_u\right) \tag{17}$$

4.3. Efficiency estimation

Various efficiencies of NPVTCPC-DS for different values of $\dot{m}_f$ and N have been estimated as follows:

4.3.1. Thermal efficiency estimation

The thermal efficiency has been estimated using first law of thermodynamics. Following Singh and Tiwari [17], the hourly, daily and annual thermal efficiencies for NPVTCPC-DS have been estimated as:

$$\eta_{\mathrm{hte}} = \frac{\left(\dot{m}_{\mathrm{ewE}} + \dot{m}_{\mathrm{ewW}}\right)\times L}{\left[\begin{array}{c}\left\{N\times\left(A_{\mathrm{am}} + A_{\mathrm{ac}}\right)\times I_b\left(t\right)\right\} + \\ \left\{\frac{A_b}{2}\left(I_{\mathrm{sE}}\left(t\right) + I_{\mathrm{sW}}\left(t\right)\right)\right\}\end{array}\right]\times 3{,}600}\times 100 \tag{18}$$

$$\eta_{\mathrm{dte}} = \frac{\sum_{t=1}^{24}\left(\dot{m}_{\mathrm{ewE}} + \dot{m}_{\mathrm{ewW}}\right)\times L}{\sum_{t=1}^{10}\left[\begin{array}{c}\left\{N\times\left(A_{\mathrm{am}} + A_{\mathrm{ac}}\right)\times I_b\left(t\right)\right\} + \\ \left\{\frac{A_b}{2}\left(I_{\mathrm{sE}}\left(t\right) + I_{\mathrm{sW}}\left(t\right)\right)\right\}\end{array}\right]\times 3{,}600}\times 100 \tag{19}$$

$$\eta_{\mathrm{ate}} = \frac{\left(\text{Annual fresh water yielding}\right)\times L}{\left(\begin{array}{c}\text{Annual heat gain + Annual solar energy} \\ \text{falling on solar still}\end{array}\right)}\times 100 \tag{20}$$

Here, one can note that hourly fresh water yielding has been integrated for 24 h to get daily fresh water yielding; whereas, heat gain as well as intensity has been integrated for 10 h only to get its daily value. The reason lies in the fact that the value of solar intensity exists for sunshine hours only; however, fresh water yielding continues to come out during night time also due to heat content of water mass.

4.3.2. Exergy efficiency estimation

The thermal exergy efficiency has been estimated using second law of thermodynamics. Following Singh and Tiwari [17], the hourly, daily and annual exergy efficiencies for NPVTCPC-DS have been estimated as:

$$\eta_{\mathrm{hte}} = \frac{\dot{\mathrm{E}}\mathrm{x}_{\mathrm{out}}}{0.933\left[\begin{array}{c}\left\{N\times\left(A_{\mathrm{am}} + A_{\mathrm{ac}}\right)\times I_b\left(t\right)\right\} + \\ \left\{\frac{A_b}{2}\times\left(I_{\mathrm{SE}}\left(t\right) + I_{\mathrm{SW}}\left(t\right)\right)\right\}\end{array}\right]}\times 100 \tag{21}$$

$$\eta_{\mathrm{dte}} = \frac{\sum_{t=1}^{24}\left[\dot{\mathrm{E}}\mathrm{x}_{\mathrm{out},d}\left(t\right)\right]}{\sum_{t=1}^{24}\left[0.933\left[\begin{array}{c}\left\{N\times\left(A_{\mathrm{am}} + A_{\mathrm{ac}}\right)\times I_b\left(t\right)\right\} + \\ \left\{\frac{A_b}{2}\times\left(I_{\mathrm{SE}}\left(t\right) + I_{\mathrm{SW}}\left(t\right)\right)\right\}\end{array}\right]\right]}\times 100 \tag{22}$$

$$\eta_{\mathrm{ate}} = \frac{\left(\text{Annual exergy output from the system}\right)}{\left(\begin{array}{c}\text{Annual exergy falling on collectors +} \\ \text{Annual exergy falling on solar still}\end{array}\right)}\times 100 \tag{23}$$

One should note here that the factor 0.933 which has been used for converting solar energy into corresponding exergy has been obtained using expression proposed by Petela [57].

4.4. Electrical efficiency estimation

The hourly, daily and yearly electrical exergy efficiencies of NPVTCPC-DS can be estimated as:

$$\eta_{\mathrm{hee}} = \frac{\dot{\mathrm{E}}\mathrm{x}_e\left(t\right) - \dot{P}_u\left(t\right)}{0.933\times A_{\mathrm{am}}\times N\times I_b\left(t\right)}\times 100 \tag{24}$$

$$\eta_{\mathrm{dee}} = \frac{\sum_{t=1}^{24}\left(\dot{\mathrm{E}}\mathrm{x}_e - \dot{P}_u\right)}{0.933\times\sum_{t=1}^{t=24}\left[A_{\mathrm{am}}\times N\times I_b\left(t\right)\right]}\times 100 \tag{25}$$

$$\eta_{\mathrm{aee}} = \frac{\left(\text{Annual electrical exergy}\right)}{\left(\begin{array}{c}\text{Annual solar exergy falling on the} \\ \text{aperture area of module of collector}\end{array}\right)}\times 100 \tag{26}$$

where $\dot{P}_u(t)$, N, $I_b(t)$ and A_{am} are hourly consumption of pump, number of collectors, beam radiation and aperture area of module respectively. The value of beam radiation and electrical energy/exergy are zero during off sunshine hours.

4.5. Overall exergy efficiency estimation

The overall exergy means the summation of thermal exergy and electrical exergy. The hourly, daily and annual overall exergy efficiencies of NPVTCPC-DS can be estimated as

$$\eta_{hoe} = \frac{\dot{E}x_{out,d}(t) + \left(\dot{E}x_e(t) - \dot{P}_u(t)\right)}{0.933 \times \left[\left[\frac{A_b}{2} \times \left(I_{SE}(t) + I_{SW}(t)\right)\right] + \left(A_{am} + A_{ac}\right) \times N \times I_b(t)\right]} \times 100 \quad (27)$$

$$\eta_{doe} = \frac{\left[\sum_{t=1}^{t=24} \dot{E}x_{out,d}(t) + \left(\dot{E}x_e(t) - \dot{P}_u(t)\right)\right]}{0.933 \times \sum_{t=1}^{24} \left[\left[\frac{A_b}{2} \times \left(I_{SE}(t) + I_{SW}(t)\right)\right] + \left(A_{am} + A_{ac}\right) \times N \times I_b(t)\right]} \times 100 \quad (28)$$

$$\eta_{ate} = \frac{\begin{pmatrix}\text{Annual overall exergy obtained from} \\ \text{NPVTCPC} - \text{DS}\end{pmatrix}}{\begin{pmatrix}\text{Annual solar exergy falling on} \\ \text{NPVTCPC} - \text{DS}\end{pmatrix}} \times 100 \quad (29)$$

4.6. Overall thermal efficiency estimation

The value of overall thermal energy can be estimated as the summation of thermal energy obtained from NPVTCPC-DS and the thermal energy equivalent to electrical exergy obtained from PVT. The electrical exergy is divided by a factor 0.38 to get the equivalent thermal energy [53]. The hourly, daily and annual overall thermal efficiencies of NPVTCPC-DS can be estimated as:

$$\eta_{hote} = \eta_{ht} + \frac{\eta_{hee}}{0.38} \quad (30)$$

$$\eta_{hote} = \eta_{dt} + \frac{\eta_{dee}}{0.38} \quad (31)$$

$$\eta_{aote} = \eta_{at} + \frac{\eta_{aee}}{0.38} \quad (32)$$

5. Methodology

The methodology to investigate the effect of $\dot{m}_f$ on various efficiencies of NPVTCPC-DS is as follows:

Step I: Taking the value of solar flux on the horizontal plane from IMD located at Pune in India, the value of solar flux on inclined plane has been evaluated using Liu and Jordan formula by computational program in MATLAB. The data for surrounding temperature has been accessed from IMD situated at Pune in India.

Step II: The computation for potable water yielding on per hour basis for different values of $\dot{m}_f$ at given N has been carried out with the help of Eq. (9) followed by the computation of potable water yielding on per year basis.

Step III: The calculation for gross energy output values at various values of $\dot{m}_f$ for given N has been performed using Eq. (10) followed by calculation for gross energy output on per year basis.

Step IV: The computation for exergy based on per hour for different values of $\dot{m}_f$ at given N has been carried out with the help of Eq. (12) followed by the calculation for exergies on per year basis. Further, gross exergy has been evaluated using Eq. (17).

Step V: The various efficiencies have been estimated using Eqs. (18)–(32) in that order.

The methodology to investigate the effect of $\dot{m}_f$ on the various efficiencies of NPVTCPC-DS at given N has been revealed as Fig. 2 for better understanding.

6. Results and discussion

The required data and all relevant equations have been fed to computational program written in MATLAB. Data on the horizontal surface has been taken from IMD Pune India. Data on the inclined surface has been evaluated using Liu and Jordan formula with the help of MATLAB. The output of programme has been presented in Figs. 3–17 and Tables 2–6.

The dissimilarity of hourly thermal efficacy and hourly exergy efficacy with $\dot{m}_f$ for NPVTCPC-DS at N = 4 and 0.14 water depth has been revealed as Figs. 3 and 4 respectively. It is clear from Figs. 3 and 4 that value of both hourly thermal and exergy efficiencies diminishes as the value of $\dot{m}_f$ is enhanced because water passing through collector does not get sufficient time to absorb heat from solar energy resulting in the addition of comparatively less amount of heat to water in the basin of NPVTCPC-DS which further results in lower rise in temperature of water in the basin. It is further seen that the value of both hourly thermal and exergy efficiencies first diminishes with the enhancement in $\dot{m}_f$ value and then become almost constant beyond $\dot{m}_f$ = 0.10 kg/s. The reason lies in the fact that the already heated water does not get further heated due to lower temperature difference between fluid and surroundings.

The dissimilarity of hourly electrical efficiency with $\dot{m}_f$ for NPVTCPC-DS at N = 4 and 0.14 m water depth has been revealed as Fig. 5. One can observe in Fig. 5 that the value of hourly electrical efficiency increases marginally with the rise in temperature due the fact that water flowing below PVT carries away heat and solar cell gets cooled. It is further seen that the value of hourly electrical exergy first increases and then become almost constant. The dissimilarity of hourly overall exergy and thermal efficiencies with $\dot{m}_f$ for NPVTCPC-DS at N = 4 has been revealed as Figs. 6 and 7. It is clear from Figs. 6 and 7 that the value of hourly overall exergy efficiency as well as hourly overall thermal efficiency decreases with the increase in $\dot{m}_f$ value and becomes almost constant beyond $\dot{m}_f$ = 0.10 kg/s. It occurs because hourly overall exergy

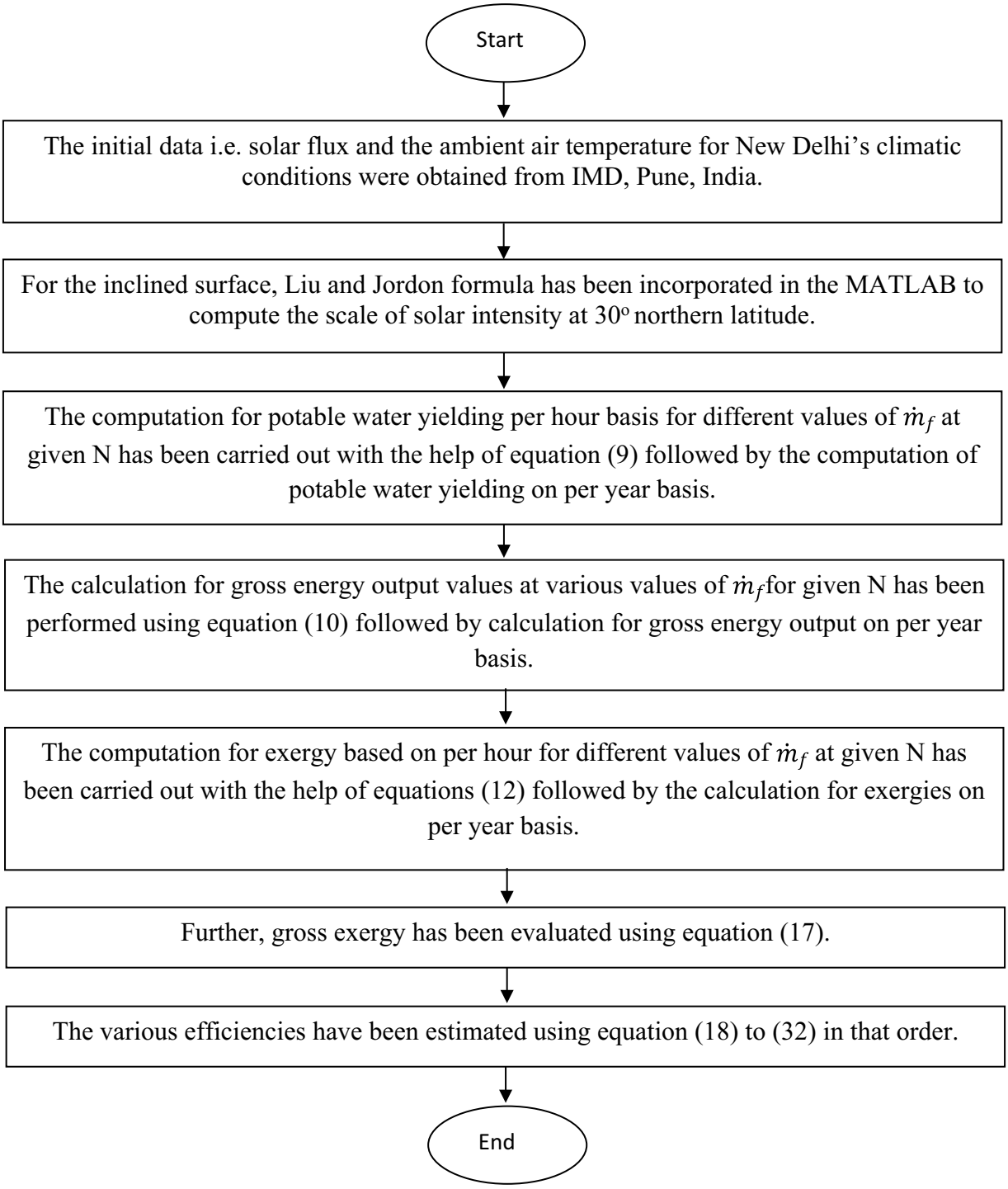

Fig. 2. Flow chart for the estimation of various efficiencies with $\dot{m}_f$ at given N for NPVTCPC-DS.

efficiency is the function of hourly exergy and hourly electrical energy. The hourly exergy and hourly electrical energy have opposite relation; however, decrease in hourly exergy overcomes the increase in hourly electrical energy and hence hourly overall exergy efficiency decreases with the increase in $\dot{m}_f$ value. Further, hourly over thermal efficiency is the function of hourly thermal efficiency and hourly electrical energy efficiency. Also, hourly thermal efficiency dominates over hourly electrical efficiency and hence the variation of hourly overall thermal efficiency follows the variation of hourly efficiency.

The variation of daily efficiencies with $\dot{m}_f$ for NPVTCPC-DS at N = 4 and 0.14 m water depth has been revealed as Fig. 8. One can observe from Fig. 8 that values of daily thermal efficiency; daily exergy efficiency, daily overall exergy efficiency and daily overall thermal efficiency

diminish with the increase in $\dot{m}_f$ value and become almost constant beyond $\dot{m}_f$ = 0.10 kg/s due to the similar variation in their corresponding hourly values. However, value of daily electrical efficiency marginally increases due to the similar variation in its hourly value.

Table 2 represents the computation of annual fresh water yielding for NPVTCPC-DS at $\dot{m}_f$ = 0.02 kg/s and N = 4. The water depth has been taken as 0.14 m. Similarly, fresh water yield at other values of $\dot{m}_f$ has been evaluated and presented as Fig. 9. It is observed from Fig. 9 that the value of fresh water yielding decreases as the value of $\dot{m}_f$ increases. It happens because water flowing through tubes of collector gets less time to absorb heat at higher value of $\dot{m}_f$. The value of fresh water yielding based on year decreases as the value of $\dot{m}_f$ increases and then it becomes almost constant because

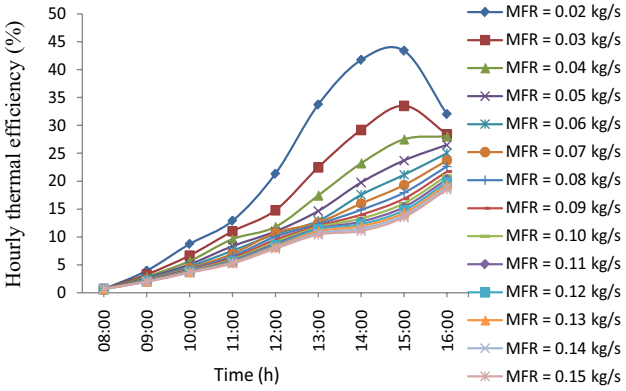

Fig. 3. Variation of hourly thermal efficiency with $\dot{m}_f$ for NPVTCPC-DS at N = 4.

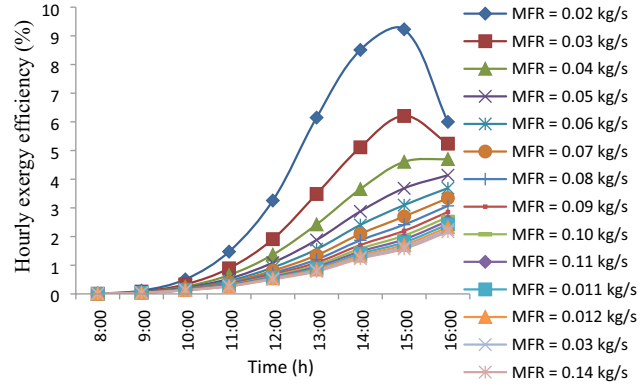

Fig. 4. Variation of hourly exergy efficiency with $\dot{m}_f$ for NPVTCPC-DS at N = 4.

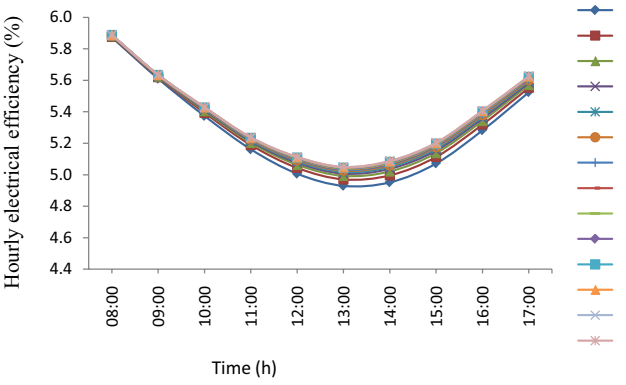

Fig. 5. Dissimilarity of hourly electrical efficiency with $\dot{m}_f$ for NPVTCPC-DS at N = 4.

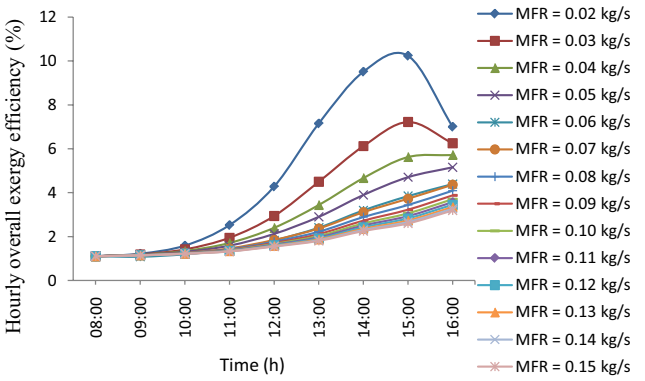

Fig. 6. Dissimilarity of hourly overall exergy efficiency with $\dot{m}_f$ for NPVTCPC-DS at N = 4.

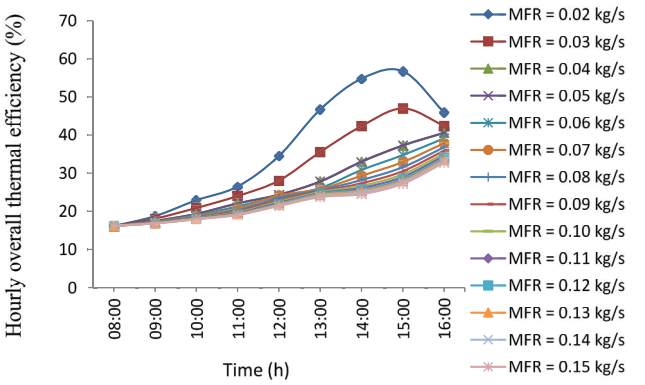

Fig. 7. Variation of hourly overall thermal efficiency with $\dot{m}_f$ for NPVTCPC-DS at N = 4.

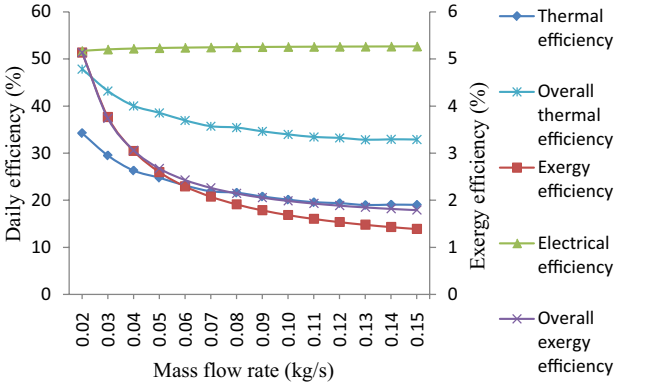

Fig. 8. Variation of daily efficiencies with $\dot{m}_f$ for NPVTCPC-DS at N = 4.

Table 2
Computation of yearly fresh water yield for NPVTCPC-DS at $\dot{m}_f$ = 0.02 kg/s, N = 4 and water depth = 0.14 m

Monthly	Daily yield	Days (Kind a)	Monthly yield (Kind a)	Daily yield	Days (Kind b)	Monthly yield (Kind b)	Daily yield	Days (Kind c)	Monthly yield (Kind c)	Daily yield	Days (Kind d)	Monthly yield (Kind d)	Gross monthly yield
Jan.	24.27	3	72.82	28.13	8	225.02	6.80	11	74.77	1.57	9	14.11	386.73
Feb.	23.23	3	69.68	22.52	4	90.06	6.87	12	82.44	1.55	9	13.91	256.09
March	25.74	5	128.69	26.65	6	159.88	11.48	12	137.76	5.57	8	44.58	470.91
April	27.79	4	111.16	27.68	7	193.79	11.64	14	162.97	9.54	5	47.72	515.64
May	27.09	4	108.36	20.72	9	186.50	13.98	12	167.75	7.95	6	47.70	510.31
June	37.02	3	111.06	20.93	4	83.72	12.24	14	171.42	4.25	6	25.48	391.67
July	22.67	2	45.34	17.63	3	52.90	12.13	10	121.26	3.56	17	60.58	280.08
Aug.	22.09	2	44.19	19.27	3	57.80	10.48	7	73.39	3.90	19	74.14	249.52
Sept.	29.23	7	204.61	25.71	3	77.14	14.24	10	142.39	5.39	10	53.87	478.02
Oct.	25.89	5	129.43	17.68	10	176.79	11.76	13	152.89	3.80	3	11.39	470.49
Nov.	23.34	6	140.01	14.75	10	147.53	5.25	12	63.00	4.30	2	8.60	359.15
Dec.	22.68	3	68.05	17.96	7	125.71	8.62	13	112.00	1.76	8	14.09	319.85
												Annual fresh water yield (kg)	4,688.47

Table 3
Computation of yearly thermal exergy for NPVTCPC-DS at $\dot{m}_f$ = 0.02 kg/s, N = 4 and water depth = 0.14 m

Daily exergy (kWh)	Days (Kind a)	Monthly exergy (Kind a) (kWh)	Daily exergy (kWh)	Days (Kind b)	Monthly exergy (Kind b) (kWh)	Daily exergy (kWh)	Days (Kind c)	Monthly exergy (Kind c) (kWh)	Daily exergy (kWh)	Days (Kind d)	Monthly exergy (Kind d) (kWh)	Gross monthly exergy (kWh)
6.39	3	19.18	5.30	8	42.39	0.71	11	7.76	0.08	9	0.69	70.03
5.55	3	16.65	5.20	4	20.80	0.65	12	7.76	0.07	9	0.60	45.81
6.24	5	31.21	6.76	6	40.54	1.32	12	15.86	0.43	8	3.42	91.03
6.53	4	26.11	6.60	7	46.19	1.25	14	17.56	0.89	5	4.44	94.29
6.10	4	24.40	3.81	9	34.31	1.83	12	21.98	0.62	6	3.69	84.38
10.26	3	30.79	4.00	4	16.00	1.31	14	18.39	0.19	6	1.14	66.31
4.84	2	9.67	3.14	3	9.42	1.39	10	13.95	0.20	17	3.32	36.36
5.08	2	10.16	4.10	3	12.29	1.01	7	7.10	0.25	19	4.76	34.31
7.79	7	54.50	6.05	3	18.16	2.06	10	20.63	0.37	10	3.66	96.95
6.63	5	33.13	3.35	10	33.51	1.60	13	20.82	0.22	3	0.67	88.13
4.62	6	27.69	2.33	10	23.34	0.41	12	4.92	0.30	2	0.60	56.56
5.39	3	16.18	3.54	7	24.77	0.97	13	12.57	0.08	8	0.67	54.19
											Annual thermal exergy output (kWh)	818.35

after certain value of $\dot{m}_f$ heat absorbed by water is very small as water flowing through tubes does not get time due to increased speed and the system behaves as working in passive mode.

The variation of annual thermal efficiency with $\dot{m}_f$ for NPVTCPC-DS at N = 4 has been revealed as Fig. 10. It is clear from Fig. 10 that the value of annual thermal efficiency diminishes as the value of $\dot{m}_f$ is increased. It has been found to occur due to the similar variation in annual fresh water yielding and hence annual thermal energy output. The value of annual thermal efficiency becomes almost constant beyond $\dot{m}_f$ = 0.10 kg/s. It occurs due to the fact that the fresh water yielding and hence energy output becomes almost constant as the water coming from collectors does add heat to basin water and further increase in temperature of basin water does not take place.

Table 3 represents the computation of yearly thermal exergy for NPVTCPC-DS at $\dot{m}_f$ = 0.02 kg/s and N = 4. The water depth has been taken as 0.14 m. Similarly, thermal exergy at other values of $\dot{m}_f$ has been evaluated and presented as Fig. 11. It is observed from Fig. 11 that values of thermal exergy decreases as the value of $\dot{m}_f$ increases. It happens because water flowing through tubes of collector gets less time to absorb heat at higher value of $\dot{m}_f$ which result in less rise in temperature of water. The value of

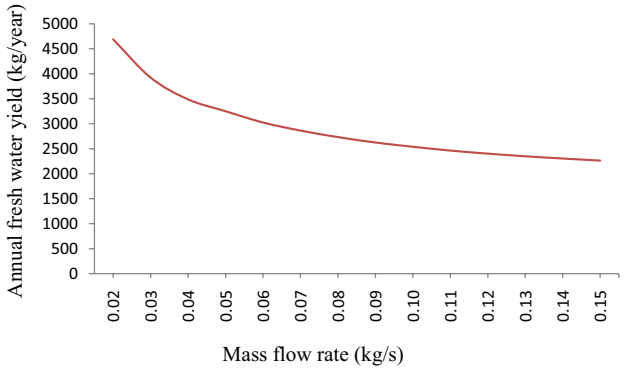

Fig. 9. Variation of Annual fresh water yielding with $\dot{m}_f$ for NPVTCPC-DS at N = 4.

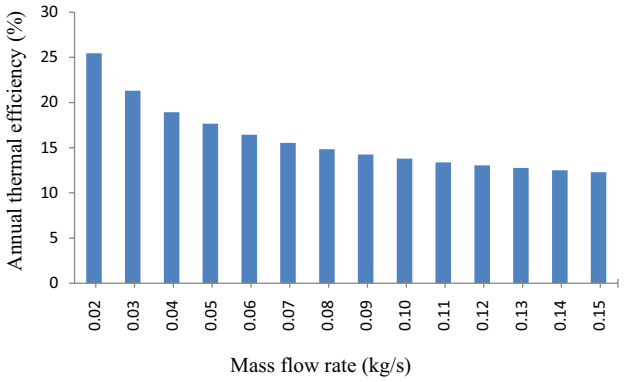

Fig. 10. Variation of annual thermal efficiency with $\dot{m}_f$ for NPVTCPC-DS at N = 4.

Table 4
Computation of yearly electrical exergy for NPVTCPC-DS at $\dot{m}_f$ = 0.02 kg/s, N = 4 and water depth = 0.14 m

Daily exergy (kWh)	Days (Kind a)	Monthly exergy (Kind a) (kWh)	Daily exergy (kW)	Days (Kind b)	Monthly exergy (Kind b) (kWh)	Daily exergy (kWh)	Days (Kind c)	Monthly exergy (Kind c) (kWh)	Daily exergy (kWh)	Days (Kind d)	Monthly exergy (Kind d) (kWh)	Gross monthly exergy (kWh)
0.646	3	1.939	0.596	8	4.769	0.309	11	3.397	0.124	9	1.114	11.219
0.616	3	1.849	0.600	4	2.401	0.299	12	3.588	0.108	9	0.968	8.807
0.597	5	2.984	0.609	6	3.652	0.339	12	4.069	0.210	8	1.677	12.381
0.566	4	2.264	0.567	7	3.967	0.301	14	4.215	0.256	5	1.279	11.724
0.523	4	2.092	0.432	9	3.890	0.317	12	3.801	0.195	6	1.173	10.956
0.670	3	2.010	0.456	4	1.825	0.284	14	3.976	0.139	6	0.833	8.644
0.495	2	0.990	0.415	3	1.244	0.302	10	3.020	0.122	17	2.077	7.331
0.510	2	1.020	0.461	3	1.382	0.262	7	1.833	0.142	19	2.689	6.924
0.561	7	3.927	0.512	3	1.536	0.337	10	3.373	0.155	10	1.547	10.383
0.552	5	2.760	0.443	10	4.435	0.342	13	4.452	0.145	3	0.434	12.081
0.546	6	3.277	0.396	10	3.959	0.211	12	2.534	0.184	2	0.368	10.138
0.588	3	1.763	0.516	7	3.611	0.337	13	4.376	0.127	8	1.013	10.763
											Annual electrical exergy output (kWh)	121.3501

thermal exergy based on year decreases as the value of $\dot{m}_f$ increases and then it becomes almost constant because after certain value of $\dot{m}_f$, heat absorbed by water is very small as water flowing through tubes does not get time due to increased speed and the system behaves as working in passive mode. The variation of annual exergy efficiency with $\dot{m}_f$ for NPVTCPC-DS at N = 4 has been revealed as Fig. 12. It is clear from Fig. 12 that the value of annual exergy efficiency decreases as the value of $\dot{m}_f$ is increased. It has been found to occur due to the similar variation in annual exergy as the input remains constant for all value of $\dot{m}_f$.

Table 4 represents the computation of yearly electrical exergy for NPVTCPC-DS at $\dot{m}_f$ = 0.02 kg/s and N = 4. The water depth has been taken as 0.14 m. Similarly, electrical exergy at other values of $\dot{m}_f$ has been evaluated and presented as Fig. 13. It is observed from Fig. 13 that values of electrical exergy increases as the value of $\dot{m}_f$ increases. It happens because water flowing through tubes of collector takes away higher amount of heat from PVT at higher value of $\dot{m}_f$ which results in decrease in temperature of solar cell. Due to decreased temperature rise of solar cell, better efficiency is obtained and hence higher electrical energy output. It is also observed that the value of electrical exergy output becomes almost constant after certain value of $\dot{m}_f$ and then it becomes almost constant. It has been found to occur because water is not able to take away heat from PVT at very high velocity of water because water does not have time to consume water. The variation of annual electrical exergy efficiency with $\dot{m}_f$ for NPVTCPC-DS at N = 4 has been revealed as Fig. 14. It is clear from Fig. 14 that the value of annual electrical exergy efficiency first increases and then it becomes almost constant beyond $\dot{m}_f$ = 0.10 kg/s due to the similar variation in the value of annual electrical exergy efficiency as the value of input remains same for all values of $\dot{m}_f$.

Figs. 15 and 16 represent the variation of annual overall energy and annual overall exergy respectively with different values of $\dot{m}_f$ for NPVTCPC-DS at water depth of 0.14 m and N = 4. It is observed from Fig. 15 that the yearly gross energy decreases as the value of $\dot{m}_f$ increases due to similar variation in yearly fresh water yielding. It is observed from Eq. (10) that the value of annual gross

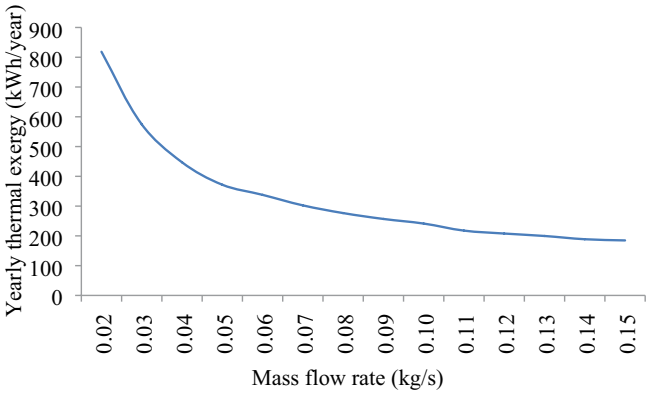

Fig. 11. Variation of annual exergy with $\dot{m}_f$ for NPVTCPC-DS at N = 4.

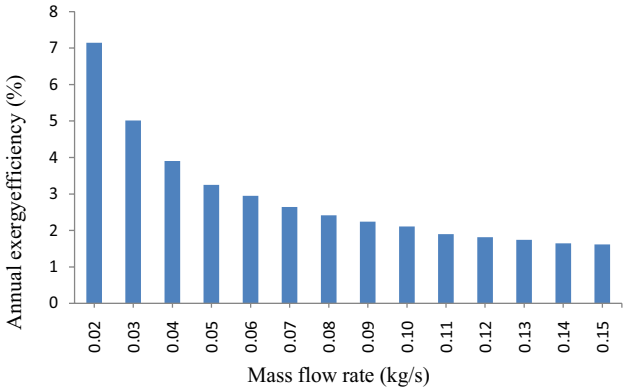

Fig. 12. Variation of annual exergy efficiency with $\dot{m}_f$ for NPVTCPC-DS at N = 4.

Table 5
Annual solar energy falling on the surface of NPVTCPC-DS for N = 4

Month	Type a			Type b			Type c			Type d			Gross MSE
	DSE	NOD	MSE	DSE	NOD	MSE	DSE	NOD	MSE	DSE	NOD	MSE	
Jan.	56.84	3	170.53	52.92	8	423.34	26.57	11	292.32	12.21	9	109.87	996.06
Feb.	55.44	3	166.31	54.39	4	217.57	26.97	12	323.59	11.85	9	106.64	814.12
March	56.65	5	283.26	58.87	6	353.23	32.40	12	388.75	22.31	8	178.47	1,203.72
April	57.20	4	228.79	57.88	7	405.16	31.71	14	443.87	28.63	5	143.15	1,220.98
May	54.88	4	219.53	46.63	9	419.68	36.03	12	432.35	24.68	6	148.10	1,219.65
June	55.05	3	165.16	48.66	4	194.64	32.89	14	460.50	19.11	9	172.03	992.34
July	50.68	2	101.37	44.03	3	132.09	32.97	10	329.72	17.28	17	293.73	856.91
Aug.	50.92	2	101.85	47.36	3	142.09	28.99	7	202.92	18.07	19	343.36	790.22
Sept.	57.83	7	404.82	52.71	3	158.13	35.60	10	355.97	18.88	10	188.82	1,107.74
Oct.	54.67	5	273.36	43.42	10	434.24	32.97	13	428.66	16.53	3	49.60	1,185.85
Nov.	52.17	6	313.00	36.82	10	368.23	20.04	12	240.49	18.00	2	35.99	957.72
Dec.	51.74	3	155.23	45.29	7	317.00	29.42	13	382.41	12.87	8	102.99	957.63
												Annual solar energy (kWh)	12,302.95

Table 6
Annual solar energy falling on the aperture are of module of NPVTCPC-DS at $N = 4$

Month	Type a			Type b			Type c			Type d			Gross MSE
	DSE	NOD	MSE	DSE	NOD	MSE	DSE	NOD	MSE	DSE	NOD	MSE	
Jan.	11.77	3	35.30	10.85	8	86.80	4.98	11	54.77	1.89	9	16.98	193.84
Feb.	11.13	3	33.40	10.77	4	43.09	4.84	12	58.13	1.65	9	14.89	149.52
March	11.05	5	55.25	11.34	6	68.01	5.74	12	68.90	3.42	8	27.36	219.52
April	10.75	4	43.02	10.78	7	75.48	5.23	14	73.20	4.39	5	21.96	213.66
May	10.10	4	40.38	8.07	9	72.61	5.69	12	68.28	3.38	6	20.30	201.57
June	10.05	3	30.16	8.35	4	33.41	4.94	14	69.17	2.31	9	20.76	153.50
July	9.24	2	18.47	7.53	3	22.60	5.27	10	52.73	2.02	17	34.33	128.13
Aug.	9.59	2	19.17	8.54	3	25.61	4.52	7	31.67	2.33	19	44.33	120.78
Sept.	11.33	7	79.30	10.07	3	30.20	6.13	10	61.27	2.63	10	26.33	197.09
Oct.	11.08	5	55.39	8.38	10	83.76	6.18	13	80.29	2.42	3	7.25	226.68
Nov.	10.79	6	64.75	7.17	10	71.71	3.55	12	42.54	3.05	2	6.10	185.10
Dec.	10.77	3	32.31	9.25	7	64.74	5.62	13	73.08	1.97	8	15.73	185.86
												Annual solar energy on aperture area of module	2,175.25

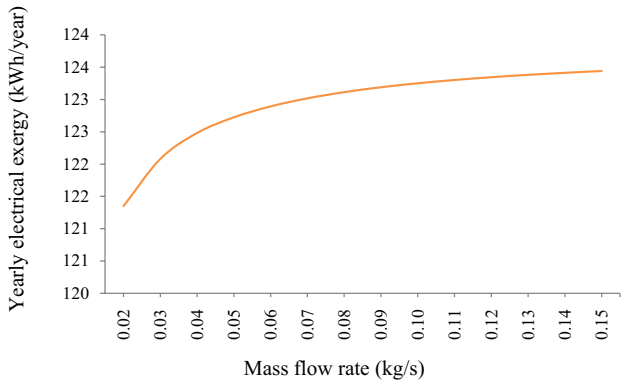

Fig. 13. Variation of annual electrical exergy with $\dot{m}_f$ for NPVTCPC-DS at $N = 4$.

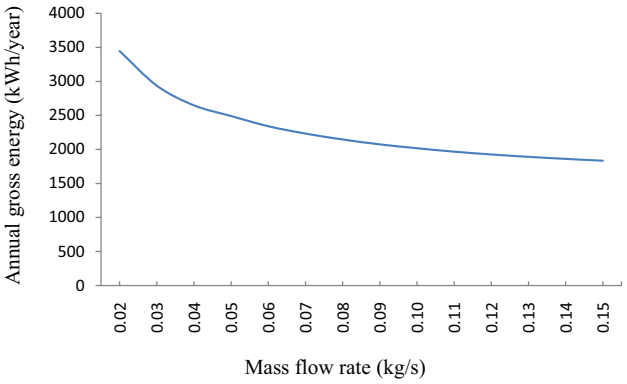

Fig. 15. Variation of annual gross energy with $\dot{m}_f$ for NPVTCPC-DS at $N = 4$.

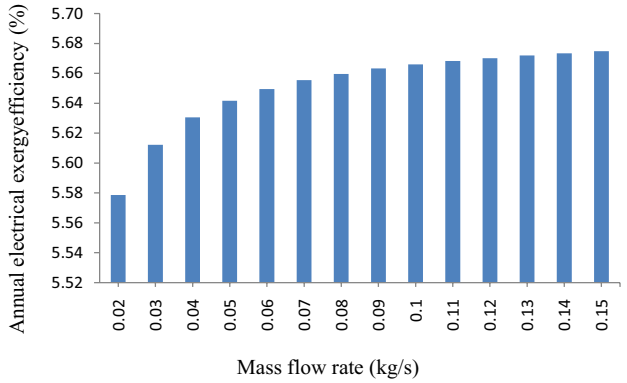

Fig. 14. Variation of annual electrical exergy efficiency with $\dot{m}_f$ for NPVTCPC-DS at $N = 4$.

energy output depends on annual energy output due fresh water yielding and annual electrical exergy. The variation in annual energy and annual electrical exergy is opposite; however, decreased annual energy output obtained due to fresh water yielding overcomes the increase in electrical exergy output with the increase in the value of $\dot{m}_f$. Hence, annual gross energy decreases with the increase in $\dot{m}_f$. Further, it is also observed from Fig. 16 that the value of annual gross exergy decreases as the value of $\dot{m}_f$ increases. It happens because the variation in annual exergy and annual electrical exergy is opposite; however, the decrease in annual thermal exergy overcome the increases in electrical energy/energy with the increase in value of $\dot{m}_f$.

The variation of annual overall exergy efficiency with $\dot{m}_f$ for NPVTCPC-DS at $N = 4$ has been revealed as Fig. 17. It is clear from Fig. 17 that the value of the value of annual overall exergy efficiency fist diminishes and then becomes almost constant beyond $\dot{m}_f = 0.10$ kg/s. It has been found to occur due to the similar variation in annual overall exergy. The variation of annual overall thermal efficiency with $\dot{m}_f$ for NPVTCPC-DS at N = 4 has been revealed as Fig. 18. It is clear from Fig. 18 that the value of overall thermal efficiency first diminishes and then becomes almost constant. It has been found to occur due to the similar variation in annual thermal efficiency because annual overall

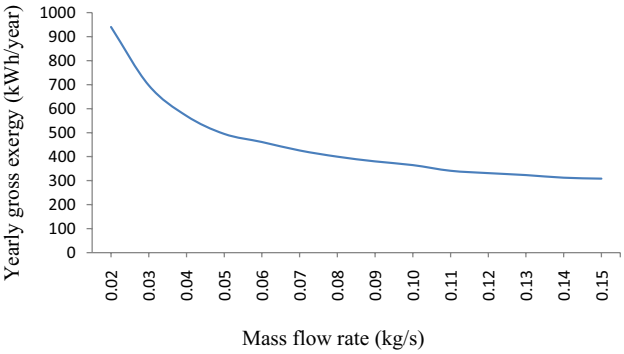

Fig. 16. Variation of annual gross exergy with $\dot{m}_f$ for NPVTF-PC-DS at $N = 4$.

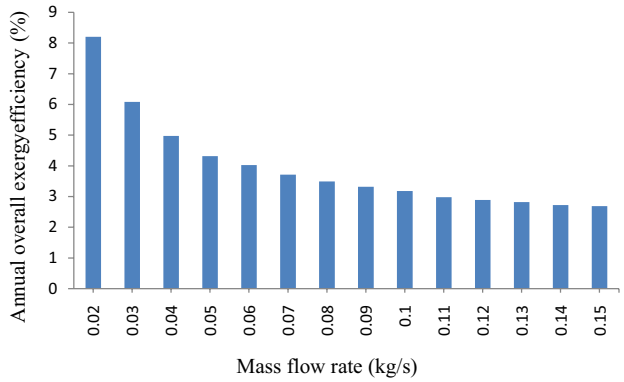

Fig. 17. Variation of annual overall exergy efficiency with $\dot{m}_f$ for NPVTCPC-DS at $N = 4$.

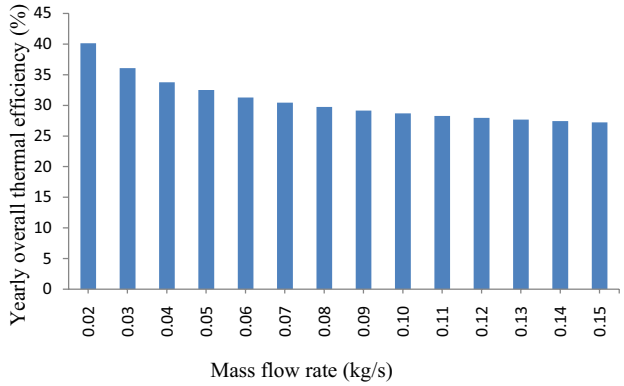

Fig. 18. Variation of annual overall thermal efficiency with $\dot{m}_f$ for NPVTCPC-DS at $N = 4$.

thermal efficiency is a function of annual thermal efficiency and annual electrical efficiency. Also, annual overall thermal energy overcomes the annual electrical energy. Hence, value of annual overall thermal efficiency diminishes first with the increase in the value of $\dot{m}_f$.

7. Conclusions

An investigation on different hourly, daily and annual efficiencies of double slope type solar still included with N similar PVT compound parabolic concentrators (NPVTCPC-DS) by incorporating dissimilarities of $\dot{m}_f$ has been carried out. Based on the current research study, the following conclusions have been made:

- Values of hourly thermal, exergy, overall exergy and overall thermal efficiencies diminish with the enhancement in $\dot{m}_f$ value; however, the value of hourly electrical efficiency increases marginally with the increase in value of $\dot{m}_f$.
- Values of daily thermal, exergy, overall exergy and overall thermal efficiencies diminish with the enhancement in $\dot{m}_f$ value and become almost constant beyond $\dot{m}_f = 0.10$ kg/s; however, the value of daily electrical efficiency increases marginally with the increase in value of $\dot{m}_f$.
- Values of annual thermal and exergy efficiencies have been found to diminish with the enhancement in the value of $\dot{m}_f$ and become almost constant beyond $\dot{m}_f = 0.10$ kg/s.
- The value of annual electrical efficiency has been found to increase with the enhancement in the value of $\dot{m}_f$ and it becomes almost constant beyond $\dot{m}_f = 0.10$ kg/s.
- Values of annual overall exergy and overall thermal efficiencies have been found to diminish with the enhancement in the value of $\dot{m}_f$ and become almost constant beyond $\dot{m}_f = 0.10$ kg/s.

Symbols

A_{rm} — Area of receiver covered by PV module, m²
A_{rc} — Area of receiver covered by glass, m²
A_{am} — Area of aperture covered by PV module, m²
A_{ac} — Area of aperture covered by glass, m²
A_{gE} — Area of east glass cover, m²
A_b — Area of basin, m²
A_{gW} — Area of west glass cover, m²
L — Latent heat, J/kg
L_g — Thickness of glass cover, m
K_g — Thermal conductivity of glass, W/m-K
$I_b(t)$ — Beam radiation, W/m²
T_a — Ambient temperature, °C
L_i — Thickness of insulation, m
K_i — Thermal conductivity of insulation, W/m-K
α_c — Absorptivity of the solar cell
$\dot{m}_f$ — Mass flow rate of water, kg/s
τ_g — Transmissivity of the glass, fraction
C_f/C_w — Specific heat of water, J/kg-K
β_o — Temperature coefficient of efficiency, K⁻¹
L_r — Total length of receiver area, m
L_a — Total length of aperture area, m
L_{rc} — Length of receiver covered by glass
L_{rm} — Length of receiver covered by PV module
L_{ac} — Length of aperture covered by glass
L_{am} — Length of aperture covered by PV module
η_c — Solar cell efficiency
η_m — PV module efficiency
η_{cN} — Temperature dependent electrical efficiency of solar cells of a number (N) of PVT-CPC water collectors
b_r — Breath of receiver, m
b_o — Breath of aperture, m

$(\alpha\tau)_{eff}$ — Product of effective absorptivity and transmittivity
F' — Collector efficiency factor
T_c — Solar cell temperature, °C
T_p — Absorber plate temperature, °C
L_p — Thickness of absorber plate, m
K_p — Thermal conductivity of absorber plate, W/m-K
T_{fi} — Fluid temperature at collector inlet, °C
T_f — Temperature of fluid in collector, °C
PF_1 — Penalty factor due to the glass covers of module
PF_2 — Penalty factor due to plate below the module
PF_3 — Penalty factor due to the absorption plate for the glazed portion
PF_c — Penalty factor due to the glass covers for the glazed portion
β — Packing factor of the module
η_o — Efficiency at standard test condition
T_{foN} — Outlet water temperature at the end of Nth PVT–CPC water collector, °C
h_i — Heat transfer coefficient for space between the glazing and absorption plate, W/m²-K
h_i' — Heat transfer coefficient from bottom of PVT to ambient, W/m²-K
h_o — Heat transfer coefficient from top of PVT to ambient, W/m²-K
U_{tca} — Overall heat transfer coefficient from cell to ambient, W/m²-K
U_{tcp} — Overall heat transfer coefficient from cell to plate, W/m²-K
h_{pf} — Heat transfer coefficient from blackened plate to fluid, W/m²-K
U_{tpa} — Overall heat transfer coefficient from plate to ambient, W/m²-K
U_{Lm} — Overall heat transfer coefficient from module to ambient, W/m²-K
U_{Lc} — Overall heat transfer coefficient from glassing to ambient, W/m²-K
P_m — Annual power generated from photovoltaic module, kWh
P_u — Annual power utilized by pump, kWh
ϵ — Emissivity
α′ — Absorptivity
$\dot{E}x$ — Hourly exergy, W
$I_{SE}(t)$ — Solar intensity on east glass cover, W/m²
$I_{SW}(t)$ — Solar intensity on west glass cover, W/m²
T_{giE} — Glass temperature at inner surface of east glass cover, °C
T_{giW} — Glass temperature at inner surface of west glass cover, °C
h_{rwg} — Radiative heat transfer coefficient from water to inner surface of glass cover, W/m²-K
h_{cwg} — Convective heat transfer coefficient from water to inner surface of glass cover, W/m²-K
h_{ewgE} — Evaporative heat transfer coefficient for east side, W/m²-K
h_{ewgW} — Evaporative heat transfer coefficient for west side, W/m²-K
M_w — Mass of water in basin, kg
$\dot{m}_{ew}$ — Mass of distillate from of double slope solar still, kg
M_{ew} — Annual yield from solar distillation system, kg
a — Clear days, blue sky
b — Hazy days, fully
c — Hazy and cloudy days, partially
d — Cloudy days, fully
$\dot{Q}_{uN}$ — The rate of useful thermal output from N identical partially (25%) covered PVT-CPC water collectors connected in series, kWh
n — Life of PVTCPC active solar distillation system, year
i — Rate of interest, %
$G_{ex,annual}$ — Overall annual exergy gain, kWh
ln — Natural logarithm
DS — Double slope
t — Time, h
R — Reflectivity
SEOWP — Solar energy operated water purifier
T_s — Temperature of sun, °C
T_w — Temperature of water in basin, °C
T_a — Ambient temperature, °C
T_{wo} — Water temperature at $t = 0$, °C
$\bar{T}_{cN}$ — Average solar cell temperature
E_{out} — Overall annual energy available from PVT-CPC solar distillation system, kWh
Ex — Daily exergy, kWh
Exm — Monthly exergy, kWh
N — Number of PVTCPC water collector
θ — Angle of inclination of glass cover with horizontal
NPVTCPC — N equal partially covered PVT compound parabolic concentrating collectors
FPC — Flat plate collector
PVT — Photovoltaic thermal
CPC — Compound parabolic concentrator
N' — Number of sunshine hours
r' — Daily diffuse to daily global irradiation ratio
η — Efficiency

Subscript

hte — Hourly thermal efficiency
dte — Daily thermal efficiency
ate — Annual thermal efficiency
g — Glass
w — Water
E — East
W — West
in — Incoming
out — Outgoing
eff — Effective

References

[1] S.N. Rai, G.N. Tiwari, Single basin solar still coupled with flat plate collector, Energy Convers. Manage., 23 (1983) 145–149.
[2] S. Kumar, A. Tiwari, An experimental study of hybrid photovoltaic thermal (PV/T) active solar still, Int. J. Energy Res., 32 (2008) 847–858.
[3] E.C. Kern, M.C. Russell, Combined Photovoltaic and Thermal Hybrid Collector Systems, Proceedings of the 13th IEEE Photovoltaic Specialists Conference, Washington, DC, USA, June 5, 1958, pp. 1153–1157.

[4] G. Singh, S. Kumar, G.N. Tiwari, Design, fabrication and performance of a hybrid photovoltaic/thermal (PVT) double slope active solar still, Desalination, 277 (2011) 399–406.
[5] D.B. Singh, J.K. Yadav, V.K. Dwivedi, S. Kumar, G.N. Tiwari, I.M. Al-Helal, Experimental studies of active solar still integrated with two hybrid PVT collectors, Sol. Energy, 130 (2016) 207–223.
[6] G.N. Tiwari, J.K. Yadav, D.B. Singh, I.M. Al-Helal, AM. Abdel-Ghany, Exergoeconomic and enviroeconomic analyses of partially covered photovoltaic flat plate collector active solar distillation system, Desalination, 367 (2015) 186–196.
[7] D.B. Singh, G.N. Tiwari, Enhancement in energy metrics of double slope solar still by incorporating N identical PVT collectors, Sol. Energy, 143 (2017) 142–161.
[8] D.B. Singh, Exergoeconomic and enviroeconomic analyses of N identical photovoltaic thermal integrated double slope solar still, Int. J. Exergy, 23 (2017) 347–366.
[9] D.B. Singh, N. Kumar, Harender, S. Kumar, S.K. Sharma, A. Mallick, Effect of depth of water on various efficiencies and productivity of N identical partially covered PVT collectors incorporated single slope solar distiller unit, Desal. Water Treat., 138 (2019) 99–112.
[10] D.B. Singh, Improving the performance of single slope solar still by including N identical PVT collectors, Appl. Therm. Eng., 131 (2018) 167–179.
[11] D.B. Singh, N. Kumar, S. Kumar, V.K. Dwivedi, J.K. Yadav, G.N. Tiwari, Enhancement in exergoeconomic and enviro-economic parameters for single slope solar still by Incorporating N Identical partially covered photovoltaic collectors, J. Sol. Energy Eng., 140 (2018) 051002 (18 p), doi: 10.1115/1.4039632.
[12] L. Sahota, G.N. Tiwari, Exergoeconomic and enviroeconomic analyses of hybrid double slope solar still loaded with nanofluids, Energy Convers. Manage., 148 (2017) 413–430.
[13] F. Carranza, C Villa, J. Aguilara, H.A. Borbón-Nuñez, D. Sauceda, Experimental study on the potential of combining TiO_2, ZnO, and Al_2O_3 nanoparticles to improve the performance of a double-slope solar still equipped with saline water preheating, Desal. Water Treat., 216 (2021) 14–33.
[14] M.R. Kouadri, N. Chennouf, M.H. Sellami, M.N. Raache, A. Benarima, The effective behavior of ZnO and CuO during the solar desalination of brackish water in southern Algeria, Desal. Water Treat., 218 (2021) 126–134.
[15] D. Atheaya, A. Tiwari, G.N. Tiwari, I.M. Al-Helal., Analytical characteristic equation for partially covered photovoltaic thermal (PVT) – compound parabolic concentrator (CPC), Sol. Energy, 111 (2015) 176–185.
[16] R. Tripathi, G.N. Tiwari, I.M. Al-Helal, Thermal modelling of N partially covered photovoltaic thermal (PVT)–Compound parabolic concentrator (CPC) collectors connected in series, Sol. Energy, 123 (2016) 174–184.
[17] D.B. Singh, G.N. Tiwari, Performance analysis of basin type solar stills integrated with N identical photovoltaic thermal (PVT) compound parabolic concentrator (CPC) collectors: a comparative study, Sol. Energy, 142 (2017) 144–158.
[18] D.B. Singh, G.N. Tiwari, Exergoeconomic, enviroeconomic and productivity analyses of basin type solar stills by incorporating N identical PVT compound parabolic concentrator collectors: a comparative study, Energy Convers. Manage., 135 (2017) 129–147.
[19] D.B. Singh, G.N. Tiwari, Effect of energy matrices on life cycle cost analysis of partially covered photovoltaic compound parabolic concentrator collector active solar distillation system, Desalination, 397 (2016) 75–91.
[20] V.S. Gupta, D.B. Singh, R.K. Mishra, S.K. Sharma, G.N. Tiwari, Development of characteristic equations for PVT-CPC active solar distillation system, Desalination, 445 (2018) 266–279.
[21] V.S. Gupta, D.B. Singh, S.K. Sharma, N. Kumar, T.S. Bhatti, G.N. Tiwari, Modeling self-sustainable fully covered photovoltaic thermal-compound parabolic concentrators connected to double slope solar distiller, Desal. Water Treat., 190 (2020) 12–27.
[22] V. Singh, D.B. Singh, N. Kumar, R. Kumar, Effect of number of collectors (N) on life cycle conversion efficiency of single slope solar desalination unit coupled with *N* identical partly covered compound parabolic concentrator collectors, Mater. Today:. Proc., 28 (2020) 2185–2189.
[23] D.B. Singh, G. Singh, N. Kumar, P.K. Singh, R. Kumar, Effect of mass flow rate on energy payback time of single slope solar desalination unit coupled with N identical compound parabolic concentrator collectors, Mater. Today:. Proc., 28 (2020) 2551–2556.
[24] G.K. Sharma, N. Kumar., D.B. Singh, A. Mallick, Exergoeconoic analysis of single slope solar desalination unit coupled with PVT-CPCs by incorporating the effect of dissimilarity of the rate of flowing fluid mass, Mater. Today:. Proc., 28 2020 2364–2368.
[25] H. Prasad, P. Kumar, R.K. Yadav, A. Mallick, N. Kumar, D.B. Singh, Sensitivity analysis of N identical partially covered (50%) PVT compound parabolic concentrator collectors integrated double slope solar distiller unit, Desal. Water Treat., 153 (2019) 54–64.
[26] K. Bharti, S. Manwal, C. Kishore, R.K. Yadav, P. Tiwar, D.B. Singh, Sensitivity analysis of n alike partly covered PVT flat plate collectors integrated double slope solar distiller unit, Desal. Water Treat., 211 (2021) 45–59.
[27] D.B. Singh, Sensitivity analysis of N identical evacuated tubular collectors integrated double slope solar distiller unit by incorporating the effect of exergy, Int. J. Exergy, 34 (2021) 424–447.
[28] K. Sampathkumar, T.V. Arjunan, P. Senthilkumar, The experimental investigation of a solar still coupled with an evacuated tube collector, Energy Sources Part A, 35 (2013) 261–270.
[29] R.V. Singh, S. Kumar, M.M. Hasan, M.E. Khan, G.N. Tiwari, Performance of a solar still integrated with evacuated tube collector in natural mode, Desalination, 318 (2013) 25–33.
[30] S. Kumar, A. Dubey, G.N. Tiwari, A solar still augmented with an evacuated tube collector in forced mode, Desalination, 347 (2014) 15–24.
[31] R.K. Mishra, V. Garg, G.N. Tiwari, Thermal modeling and development of characteristic equations of evacuated tubular collector (ETC), Sol. Energy, 116 (2015) 165–176.
[32] D.B. Singh, V.K. Dwivedi, G.N. Tiwari, N. Kumar, Analytical characteristic equation of N identical evacuated tubular collectors integrated single slope solar still, Desal. Water Treat., 88 (2017) 41–51.
[33] D.B. Singh, G.N. Tiwari, Analytical characteristic equation of N identical evacuated tubular collectors integrated double slope solar still, J. Solar Energy Eng.: Include. Wind Energy Build. Energy Conserv., 135 (2017) 051003 (1–11).
[34] D.B. Singh, G.N. Tiwari, Energy, exergy and cost analyses of N identical evacuated tubular collectors integrated basin type solar stills: a comparative study, Sol. Energy, 155 (2017) 829–846.
[35] R.J. Issa, B. Chang, Performance study on evacuated tubular collector coupled solar still in West Texas climate, Int. J. Green Energy, 14 (2017) 793–800.
[36] D.B. Singh, I.M. Al-Helal, Energy metrics analysis of N identical evacuated tubular collectors integrated double slope solar still, Desalination, 432 (2018) 10–22.
[37] D.B. Singh, N. Kumar, A. Raturi, G. Bansal, A. Nirala, N. Sengar, Effect of Flow of Fluid Mass Per Unit Time on Life Cycle Conversion Efficiency of Double Slope Solar Desalination Unit Coupled with N Identical Evacuated Tubular Collectors, Lecture Notes in Mechanical Engineering, Advances in Manufacturing and Industrial Engineering, Select Proceedings of ICAPIE 2019, 2021, pp. 393–402.
[38] S.K. Sharma, D.B. Singh, A. Mallick, S.K. Gupta, Energy metrics and efficiency analyses of double slope solar distiller unit augmented with N identical parabolic concentrator integrated evacuated tubular collectors: a comparative study, Desal. Water Treat., 195 (2020) 40–56.
[39] S.K. Sharma, A. Mallick, S.K. Gupta, N. Kumar, D.B. Singh, G.N. Tiwari, Characteristic equation development for double slope solar distiller unit augmented with N identical parabolic concentrator integrated evacuated tubular collectors, Desal. Water Treat., 187 (2020) 178–194.

[40] R.V. Patel, K. Bharti, G. Singh, R. Kumar, S. Chhabra. D.B. Singh, Solar still performance investigation by incorporating the shape of basin liner: a short review, Mater. Today:. Proc., 43 (2021) 597–604.
[41] R.V. Patel, K. Bharti, G. Singh, G. Mittal, D.B. Singh, A. Yadav, Comparative investigation of double slope solar still by incorporating different types of collectors: a mini review, Mater. Today:. Proc., 38 (2021) 300–304.
[42] R.V. Patel, G. Singh, K. Bharti, R. Kumar, D.B. Singh, A mini review on single slope solar desalination unit augmented with different types of collectors, Mater. Today:. Proc., 38 (2021) 204–210.
[43] G. Singh, D.B. Singh, S. Kumara, K. Bharti, S. Chhabra, A review of inclusion of nanofluids on the attainment of different types of solar collectors, Mater. Today:. Proc., 38 (2021), 153–159.
[44] G. Bansal, D.B. Singh, C. Kishore, V. Dogra, Effect of Absorbing Material on the performance of solar still: a mini review, Mater. Today:. Proc., 26 (2020) 1884–1887.
[45] P. Shankar, A. Dubey, S. Kumar, G.N. Tiwari, Production of clean water using ETC integrated solar stills: thermoenviro-economic assessment, Desal. Water Treat., 218 (2021) 106–118.
[46] S. Abdallah, M. Nasir, D. Afaneh, Performance evaluation of spherical and pyramid solar stills with chamber stepwise basin, Desal. Water Treat., 218 (2021) 119–125.
[47] F.A. Essa, F.S. Abou-Taleb, M.R. Diab, Experimental investigation of vertical solar still with rotating discs, Energy Sources, Part A, (2021) 1950238, doi: 10.1080/15567036.2021.1950238.
[48] M.A. Elaziz, F.A. Essa, A.H. Elsheikh, Utilization of ensemble random vector functional link network for freshwater prediction of active solar stills with nanoparticles, Sustainable Energy Technol. Assess., 47 (2021) 101405, doi: 10.1016/j.seta.2021.101405.
[49] H. Hassan, M.S. Yousef, M. Fathy, M.S. Ahmede, Assessment of parabolic trough solar collector assisted solar still at various saline water mediums via energy, exergy, exergoeconomic, and enviroeconomic approaches, Renewable Energy, 155 (2020) 604–616.
[50] A.K. Thakur, R. Sathyamurthy, R. Velraj, I. Lynch, R. Saidur, A.K. Pandey, S.W. Sharshir, Z. Ma, P.G. Kumar, A.E. Kabeel, Sea-water desalination using a desalting unit integrated with a parabolic trough collector and activated carbon pellets as energy storage medium, Desalination, 516 (2021) 115217, doi: 10.1016/j.desal.2021.115217.
[51] D.L. Evans, Simplified method for predicting PV array output, Sol. Energy, 27 (1981) 555–560.
[52] T. Schott, Operational Temperatures of PV Modules, Proceedings of 6th PV Solar Energy Conference, 1985, pp. 392–396.
[53] B.J. Huang, T.H. Lin, W.C. Hung, F.S. Sun, Performance evaluation of solar photovoltaic/thermal systems, Sol. Energy, 70 (2001) 443–448.
[54] P.K. Nag, Basic and Applied Thermodynamics, Tata McGraw-Hill, ISBN 0-07-047338-2, 2004.
[55] P.I. Cooper, Digital simulation of experimental solar still data, Sol. Energy, 14 (1973) 451.
[56] R.V. Dunkle, Solar Water Distillation, the Roof Type Solar Still and Multi Effect Diffusion Still, International Developments in Heat Transfer, A.S.M.E., Proceedings of International Heat Transfer, Part V, University of Colorado, 1961, p. 895.
[57] R. Petela, Exergy of undiluted thermal radiation, Sol. Energy, 86 (2003) 241–247.

Appendix-A

Expressions for various terms used in Eqs. (1) and (2) are as follows.

$$U_{\text{tca}} = \left[\frac{1}{h_o} + \frac{L_g}{K_g}\right]^{-1};\quad U_{\text{tcp}} = \left[\frac{1}{h_i} + \frac{L_g}{K_g}\right]^{-1};$$

$$h_o = 5.7 + 3.8V,\quad \text{Wm}^{-2}\text{K}^{-1};\quad h_i = 5.7, \text{Wm}^{-2}\text{K}^{-1};$$

$$U_{\text{tpa}} = \left[\frac{1}{U_{\text{tca}}} + \frac{1}{U_{\text{tcp}}}\right]^{-1} + \left[\frac{1}{h_i'} + \frac{1}{h_{\text{pf}}} + \frac{L_i}{K_i}\right]^{-1};\quad h_{\text{pf}} = 100\ \text{Wm}^{-2}\text{K}^{-1}$$

$$h_i' = 2.8 + 3V',\quad \text{Wm}^{-2}\text{K}^{-1};$$

$$U_{L1} = \frac{U_{\text{tcp}}U_{\text{tca}}}{U_{\text{tcp}} + U_{\text{tca}}},\quad U_{L2} = U_{L1} + U_{\text{tpa}};\quad U_{\text{Lm}} = \frac{h_{\text{pf}}U_{L2}}{F'h_{\text{pf}} + U_{L2}};$$

$$U_{\text{Lc}} = \frac{h_{\text{pf}}U_{\text{tpa}}}{F'h_{\text{pf}} + U_{\text{tpa}}};$$

$$\text{PF}_1 = \frac{U_{\text{tcp}}}{U_{\text{tcp}} + U_{\text{tca}}};\quad \text{PF}_2 = \frac{h_{\text{pf}}}{F'h_{\text{pf}} + U_{L2}};\quad \text{PF}_c = \frac{h_{\text{pf}}}{F'h_{\text{pf}} + U_{\text{tpa}}};$$

$$(\alpha\tau)_{\text{1eff}} = \rho(\alpha_c - \eta_c)\tau_g\beta_c\frac{A_{\text{am}}}{A_{\text{rm}}};\quad (\alpha\tau)_{\text{2eff}} = \rho\alpha_p\tau_g^2(1-\beta_c)\frac{A_{\text{am}}}{A_{\text{rm}}};$$

$$(\alpha\tau)_{\text{meff}} = \left[(\alpha\tau)_{\text{1eff}} + \text{PF}_1(\alpha\tau)_{\text{2eff}}\right];(\alpha\tau)_{\text{ceff}} = \text{PF}_c\cdot\rho\alpha_p\tau_g\frac{A_{\text{ac}}}{A_{\text{rc}}};$$

$$A_{\text{rm}} = b_r L_{\text{rm}};\quad A_{\text{am}} = b_o L_{\text{am}};$$

$$A_cF_{\text{Rc}} = \frac{\dot{m}_f c_f}{U_{\text{Lc}}}\left[1 - \exp\left(\frac{-F'U_{\text{Lc}}A_c}{\dot{m}_f c_f}\right)\right.$$

$$A_mF_{\text{Rm}} = \frac{\dot{m}_f c_f}{U_{\text{Lm}}}\left[1 - \exp\left(\frac{-F'U_{\text{Lm}}A_m}{\dot{m}_f c_f}\right)\right];$$

$$\left(AF_R(\alpha\tau)\right)_1 = \left[A_cF_{\text{Rc}}(\alpha\tau)_{\text{ceff}} + PF_2(\alpha\tau)_{\text{meff}}A_mF_{\text{Rm}}\left(1 - \frac{A_cF_{\text{Rc}}U_{\text{Lc}}}{\dot{m}_f c_f}\right)\right];$$

$$\left(AF_RU_L\right)_1 = \left[A_cF_{\text{Rc}}U_{\text{Lc}} + A_mF_{\text{Rm}}U_{\text{Lm}} + A_mF_{\text{Rm}}U_{\text{Lm}}\left(1 - \frac{A_cF_{\text{Rc}}U_{\text{Lc}}}{\dot{m}_f c_f}\right)\right]$$

$$K_K = \left(1 - \frac{\left(AF_RU_L\right)_1}{\dot{m}_f c_f}\right)$$

$$\left(AF_R(\alpha\tau)\right)_{m1} = PF_2(\alpha\tau)_{\text{meff}}A_mF_{\text{Rm}}$$

$$\left(AF_RU_L\right)_{m1} = A_mF_{\text{Rm}}U_{\text{Lm}}$$

$$K_m = \left(1 - \frac{A_mF_{\text{Rm}}U_{\text{Lm}}}{\dot{m}_f c_f}\right)$$

Expressions for various terms used in Eqs. (4)–(15) are as follows.

$$a = \frac{1}{M_wC_w}\left[\dot{m}_fC_f\left(1 - K_k^N\right) + U_bA_b + \frac{h_{\text{1wE}}\left(P - A_2\right)A_b}{2P} + \frac{h_{\text{1wW}}\left(P - B_2\right)A_b}{2P}\right];$$

$$\bar{f}(t)=\frac{1}{M_w C_w}\left[\left(\frac{\alpha'_w}{2}+h_1\alpha'_b\right)A_b\left(\bar{I}_{SE}(t)+\bar{I}_{SW}(t)\right)+\frac{\left(1-K_k^N\right)}{\left(1-K_k\right)}\left(AF_R(\alpha\tau)\right)_1\bar{I}_b(t)+\left(\frac{\left(1-K_k^N\right)}{\left(1-K_k\right)}\left(AF_RU_L\right)_1+U_bA_b\right)T_a+\left(\frac{h_{1wE}A_1+h_{1wW}B_1}{P}\right)\frac{A_b}{2}\right];$$

$$A_1=R_1U_1A_{gE}+R_2h_{EW}A_{gW}$$

$$A_2=h_{1WE}U_2\frac{A_b}{2}+h_{EW}h_{1WW}\frac{A_b}{2}$$

$$P=\left(U_1U_2-\frac{h_{EW}^2}{A_{gE}}h_{1WW}\frac{A_b}{2}\right)A_{gW}$$

$$U_1=\frac{h_{1wE}\frac{A_b}{2}+h_{EW}A_{gE}+U_{c,gaE}A_{gE}}{A_{gW}}$$

$$U_2=\frac{h_{1wW}\frac{A_b}{2}+h_{EW}A_{gW}+U_{c,gaW}A_{gW}}{A_{gE}}$$

$$B_1=\frac{\left(R_2P+A_1h_{EW}\right)A_{gW}}{U_2A_{gE}}$$

$$B_2=\frac{Ph_{1wW}\frac{A_b}{2}+h_{EW}A_{gW}A_2}{U_2A_{gE}}$$

$$R_1=\alpha'_g\,I_{SE}(t)+U_{c,gaE}T_a$$

$$R_2=\alpha'_g\,I_{SW}(t)+U_{c,gaW}T_a$$

$$h_{EW}=0.034\times5.67\times10^{-8}\left[\left(T_{giE}+273\right)^2+\left(T_{giW}+273\right)^2\right]\left[T_{giE}+T_{giW}+546\right]$$

$$U_{c,gaE}=\frac{\frac{K_g}{l_g}h_{1gE}}{\frac{K_g}{l_g}+h_{1gE}};\quad U_{c,gaW}=\frac{\frac{K_g}{l_g}h_{1gW}}{\frac{K_g}{l_g}+h_{1gW}};$$

$$h_{1gE}=5.7+3.8V;\quad h_{1gW}=5.7+3.8V;$$

$$h_{1wE}=h_{rwgE}+h_{cwgE}+h_{ewgE}$$

$$h_{1wW}=h_{rwgW}+h_{cwgW}+h_{ewgW}$$

$$h_{e,wgE}=16.273\times10^{-3}h_{c,wgE}\left[\frac{P_w-P_{giE}}{T_w-T_{giE}}\right];$$

$$h_{c,wgE}=0.884\left[\left(T_w-T_{giE}\right)+\frac{\left(P_w-P_{gi}E\right)\left(T_w+273\right)}{268.9\times10^3-P_w}\right]^{\frac{1}{3}};$$

$$h_{c,wgW}=0.884\left[\left(T_w-T_{giW}\right)+\frac{\left(P_w-P_{giW}\right)\left(T_w+273\right)}{268.9\times10^3-P_w}\right]^{\frac{1}{3}};$$

$$P_w=\exp\left[25.317-\frac{5{,}144}{T_w+273}\right];$$

$$P_{giE}=\exp\left[25.317-\frac{5{,}144}{T_{giE}+273}\right];$$

$$P_{giW}=\exp\left[25.317-\frac{5{,}144}{T_{giW}+273}\right];$$

$$h_{rwgE}=\left(0.82\times5.67\times10^{-8}\right)\left[(T_w+273)^2+(T_{giE}+273)^2\right]\left[T_w+T_{giE}+546\right];$$

$$h_{rwgW}=\left(0.82\times5.67\times10^{-8}\right)\left[\left(T_w+273\right)^2+\left(T_{giW}+273\right)^2\right]\left[T_w+T_{giW}+546\right];$$